DoE/ER/45271--T6

DOE/ER/45271--T6

DE93 008635

II. Progress and Accomplishments During the Period of the Previous DOE Grant No. DE-FG02-86-ER45271.A

The present grant period (since August 1989) has been one of rapid progress and development of the new field of molecular/polymeric magnets. A list of publications as well as invited and contributed presentations that have resulted from our studies under this grant is presented in Appendix A.

Our accomplishments during this past grant period span three areas of research. (i) Following models we and others have proposed, we have synthesized numerous new materials to test the generality of magnetism in molecular/polymeric systems. This activity is capped by our disclosure of the first room temperature molecular based magnet $V(TCNE)_x$ y(solvent). (ii) We have extensively studied the ferromagnetic transition and related transitions in decamethylferrocenium tetracyanoethanide, $[FeCp^*_2][TCNE]$, Figure 1, $V(TCNE)_x$

y(solvent), and related materials. (iii) We have tested ours and others' models for ferromagnetic and antiferromagnetic exchange between local sites, and models for control of T_C, determining successes and shortcomings. We briefly summarize here the major breakthroughs, accomplishments, and discoveries that have occurred during this period:

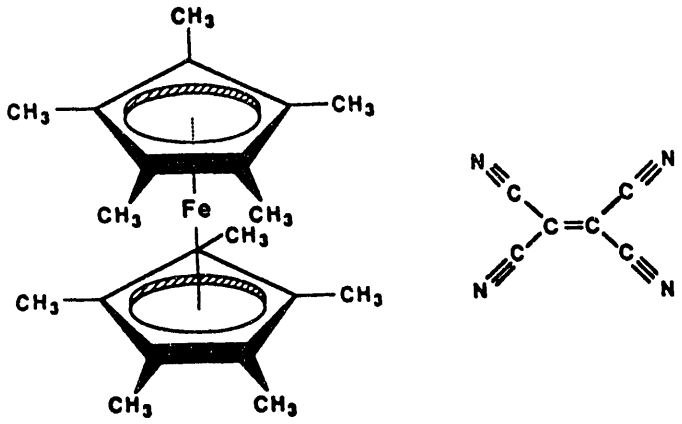

Figure 1. (a) $FeCp^*_2$, (b) TCNE

(i) Synthesis and chemical and structural characterization of new magnets

- *Synthesis of the first room temperature molecular/organic-based magnet* $V(TCNE)_x \cdot y(CH_2Cl_2)$. A new polymeric material was synthesized by reacting the vanadium organometallic compound bis(benzene)vanadium(0), and the organic acceptor tetracyanoethylene (TCNE) [6]. The reaction product is an insoluble amorphous black solid which exhibits field dependent magnetization, Figure 2, and hysteresis, Figure 3, demonstrating that it is a room temperature magnet. The critical temperature exceeds 350K, the thermal decomposition temperature of the material. Empirical composition of the reported material is $V(TCNE)_x \cdot y(CH_2Cl_2)$ with x~2 and y~1/2. This new magnet is stable when protected from the atmosphere.

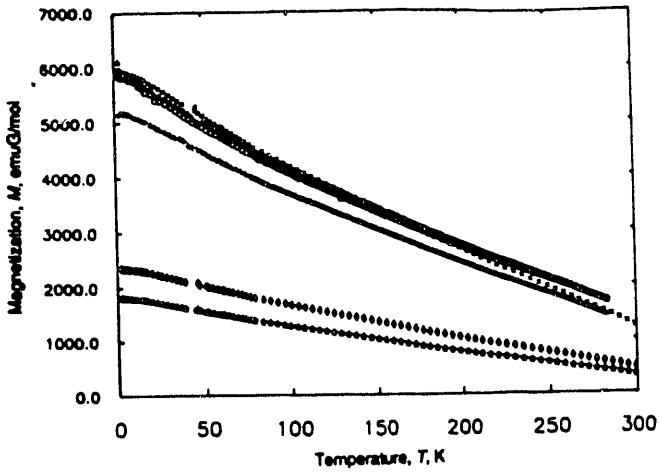

Figure 2. Magnetization *M* as a function of temperature *T* at 19.5 (O), 15.8 (Δ), 5.25 (+), 2.0 (x), 0.5. (◊), and 0.15 (*) kG for $V(TCNE)_x{\cdot}y(CH_2Cl_2)$.

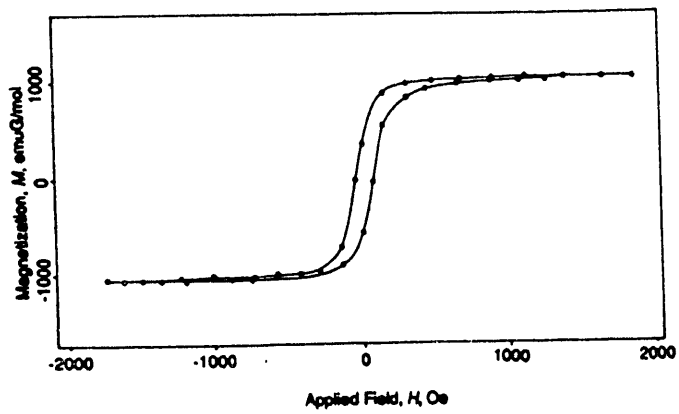

Figure 3. Hysteresis *M(H)* of $V(TCNE)_x{\cdot}y(CH_2Cl_2)$ at room temperature (the data were taken on a vibrating sample magnetometer). The line is a guide for the eye.

- *Developed a model of local structural order in $V(TCNE)_x{\cdot}y(CH_2Cl_2)$.* Infrared analysis is consistent with each vanadium being coordinated with up to 6 ligands (primarily N's from different TCNE's in an expected octahedral-like environment). Chlorine from the weak CH_2Cl_2 ligand or from the oxidative addition of CH_2Cl_2 may also enter the coordination sphere. Figure 4 illustrates some of the likely bonding in this structure which has only short-range order.
- *Synthesized variants of $V(TCNE)_x{\cdot}y(CH_2Cl_2)$* The synthesis of V/X with X=TCNQ, $TCNQF_4$, $C_4(CN)_6$, chloranil, cyanil, and DDQ has been achieved; however all of these materials are paramagnetic in their behavior, Figure 5. The V/TCNQ system requires further exploration due to evidence for ferromagnetic coupling. The V/TCNE magnet has been prepared in other solvents (e.g., Et_2O, THF, CH_3CN). The use of coordinating solvents results in a suppressed T_c, Figure 6. This supports the important role of coordination of the organic moiety in determining the three-dimensional cooperative behavior.

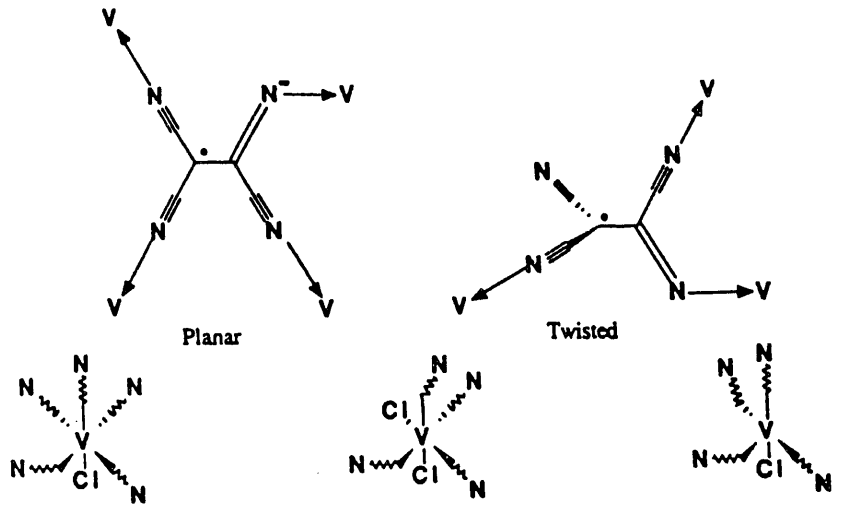

Figure 4. Proposed local bonding about each TCNE and V.

- *Developed "alloys" of spinless $[CoCp^*_2]^{+\cdot}$ and spin 1/2 $[FeCp^*_2]^{+\cdot}$ containing metallocene electron-transfer salts, $[FeCp^*_2]^{+\cdot}y[CoCp^*_2]^{+}1\text{-}y$ $[TCNE]^{-\cdot}$.* This enabled the quantitative study of the effects of spin dilution and oligomer size in anisotropic magnets.
- *Prediction of scaling of T_C with increase of magnitude of spin.*
- *Synthesized mixed S=1 and S=1/2 electron transfer salt $[MnCp^*_2]^{+:}$ $[TCNE]^{-\cdot}$.* This compound made possible a test of the predictions of the role of spin magnitude on T_C.
- *Synthesized model mixed spin compounds based on $[MnCp^*_2]^{+:}[DDQ]^{-\cdot}$.* This system was the basis of a study to test the role of interchain exchange.

ii. Magnetic Studies

- *Magnetization studies of $V(TCNE)_x{\cdot}y(CH_2Cl_2)$.* Spin wave theory analysis of low temperature (T< 60K) magnetization M for $V(TCNE)_x{\cdot}y(C^1H_2Cl_2)$ Figure 7, was carried out. Model analysis ($[M(T=0)-M(T)] = AT^{3/2}$, where A is a constant) yields a prediction of $T_C \approx 400K$, in agreement with observed $T_C > 350K$ (thermal decomposition temperature) and linear extrapolation of M(T) to zero. Quantitative mean field analysis of magnetization, Figure 8, required introduction of disorder and the effects of a "third" sublattice.

  Extrapolation of these mean field analyses to high temperature also predicts $T_C \approx 400K$.

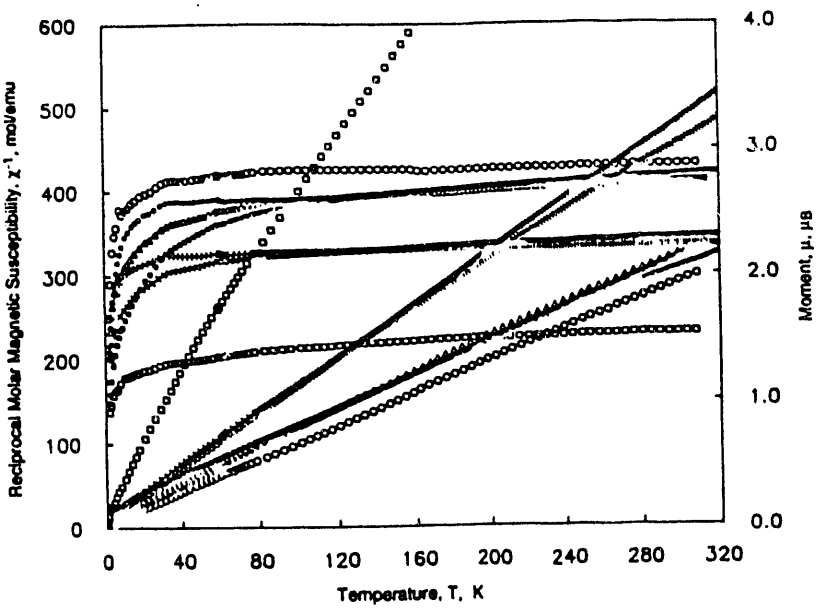

Figure 5. Reciprocal magnetic susceptibility and moment for the black precipitate arising from the reaction of $V^0(C_6H_6)_2$ and TCNQ (o), $TCNQF_4$ (●), $C_4(CN)_6$ (+), chloranil (□), cyanil (■), TCNE from Me_4THF (Δ) and DDQ (×) in CH_2Cl_2.

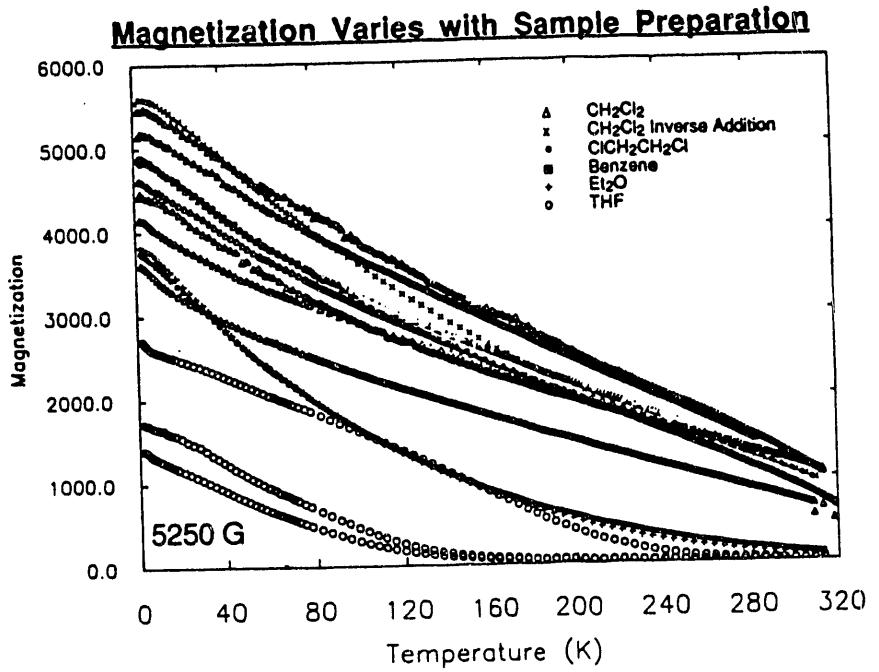

Figure 6. Magnetization (emu/G mole) vs temperature (K) of $V(TCNE)_x y(solvent)$ for samples in CH_2Cl_2 (Δ, x), $ClCH_2CH_2Cl$ (●), benzene (■), Et_2O (+) and THF (o) solvents.

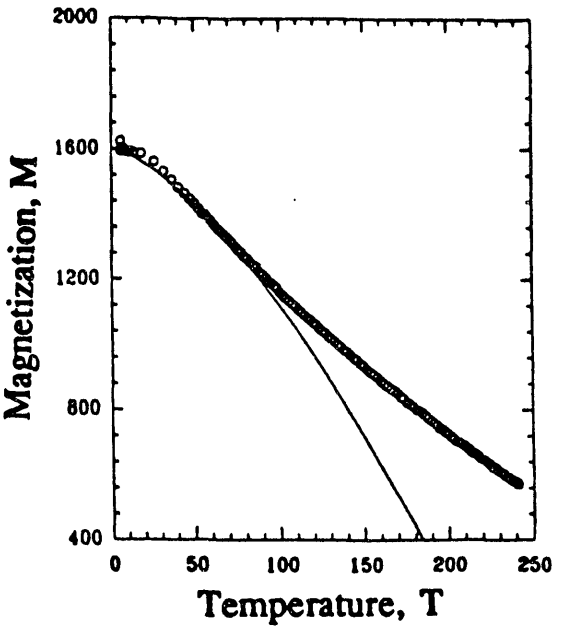

Figure 7. Zero applied magnetic field magnetization (emu G/mole) vs. temperature (K) for V/TCNE/CH_2C_2 (o). The solid curve is a fit to spin wave theory ($M(T)-M(0) = AT^{3/2}$).

- *Discovery of spin glass behavior at low temperatures in $V(TCNE)_x \cdot y(coordinating\ solvent)$.* Ac susceptibility of $V(TCNE)_x \cdot y(CH_3CN)$ indicates a transition from the paramagnetic state to a ferrimagnetic state at $T_C \sim 65K$ with a second transition to a spin glass state at $T_f \sim 15K$, Figure 9. It is hypothesized that this unusual spin glass behavior results from coordination of the nonmagnetic CH_3CN solvent with V. This introduces increased disorder in the local spin exchange environment thereby producing a stable spin glass state at low temperatures.
- *First demonstration of the essential role of anisotropy of exchange in determining T_C of ferromagnets through spin dilution studies of $[FeCp^*_2]^{+\cdot}{}_x[CoCp^*_2]^{+}{}_{1-x}[TCNE]^{-\cdot}$.* The ordering temperature T_C decreased rapidly with concentration of spinless sites, Figure 10.

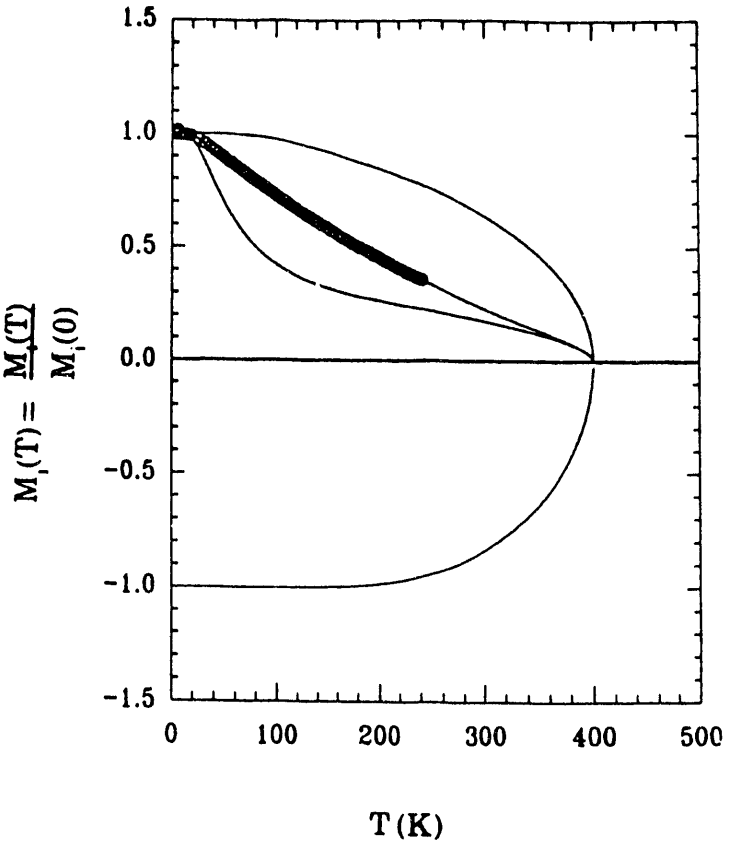

Figure 8. Mean field analysis of zero field magnetization vs. temperature for V/TCNE/CH_2Cl_2. Open circle are the zero applied magnetic magnetization vs. temperature. The three solid lines represent the normalized contributions of V^{2+} (S = 3/2) antiferromagnetically coupled to S = 1/2 $TCNE^-$ (top and bottom solid curves, respectively, $J_{V/TCNE} \approx -265$) and S = 1/2 $TCNE^-$ antiferromagnetically on to other $TCNE^-$ ($J_{TCNE/TCNE} \approx -65$K, with effective ferromagnetic coupling to V of + 43,5K).

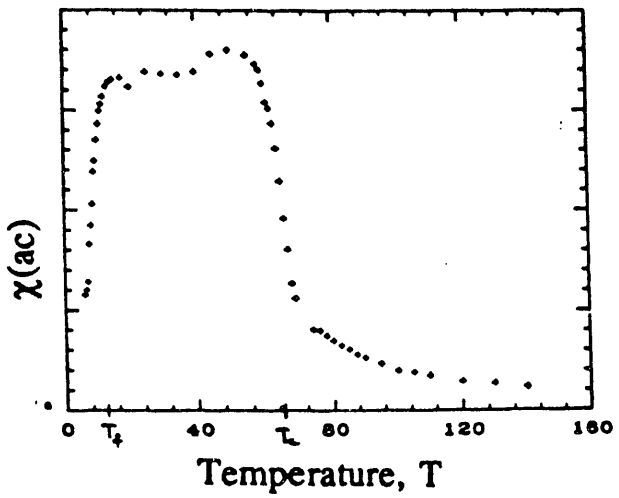

Figure 9. Real part of ac susceptibility (arbitrary units) vs temperature (K).

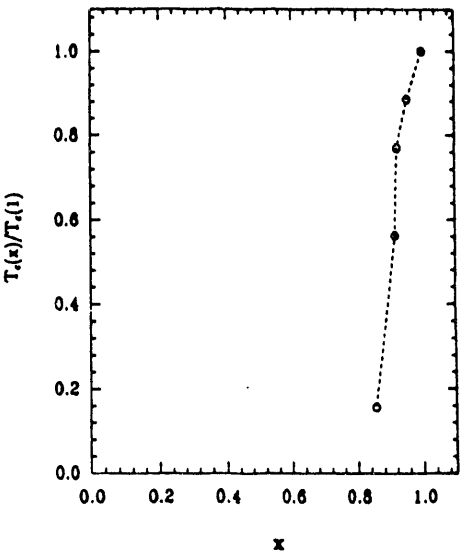

Figure 10. $T_c(X)/T_c(x=1)$ vs x for $[FeCp^*_2]_x[CoCp^*_2]_{1-x}[TCNE]$.

- *The electron-transfer salt $[MnCp^*_2]^{+\cdot}[TCNE]^{-\cdot}$ was shown to be a ferromagnet with T_C = 8.8K.* This is the highest ferromagnetic T_C for a metallocene-based system yet reported, Figure 11.

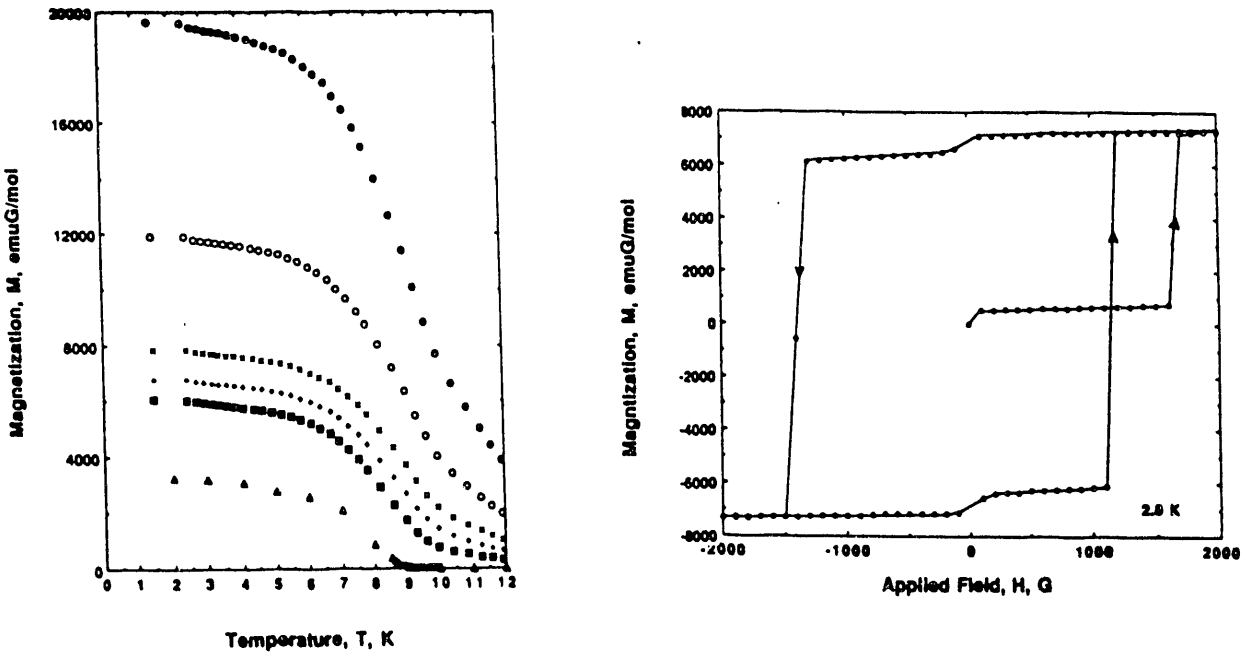

(a) (b)

Figure 11. (a) Magnetization, *M*, as a function of temperature in decreasing order for a 19.5 kG cooled microcrystalline sample of $[MnCp^*_2]^{\cdot+}[TCNE]^{\cdot-}$ previously aligned in 19.5 kG at 2000 (•), 1000 (o), 500 (x), 300 (+), 150 (■); (b) hysteresis data at 2.0K.

- *Metamagnetic behavior discovered in $[MnCp^*_2]^{+\cdot}[DDQ]^{-\cdot}$ below its Néel temperature of 8.8K.* Anomalous magnetic behavior occurs below 4K in the form of large hysteresis and remanent moment, Figure 12. An equilibrium phase diagram and unique set of two nonequilibrium phase diagrams were derived, Figure 12C.

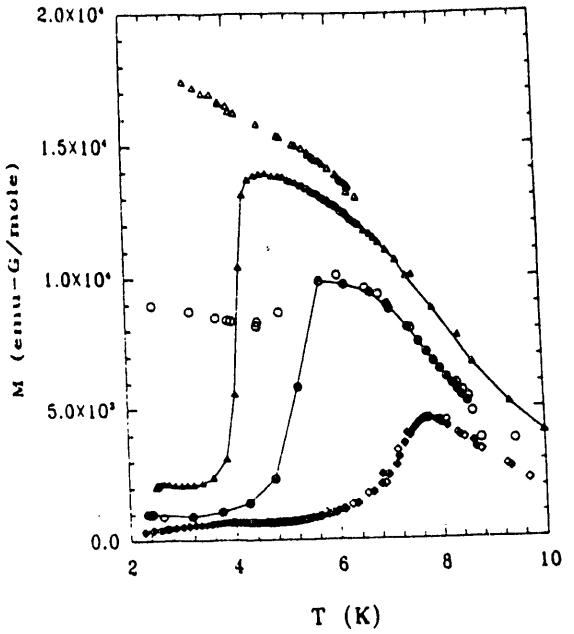

Figure 12 (A). $M_1(T)$ of $[MnCp^*_2][DDQ]$ for differing H. Open symbols symbols represent data collected while cooling and warming aligned samples after the magnetic field was changed at high temperature ($>T_N$): 1000 G Δ, 788 G ○, and 551 G ◇; the solid symobls represent results for zero field cooled samples, magnetic field was changed at 2K, and data collected while warming: 1000 G ▲, 788 G ●, and 551 G ◆.

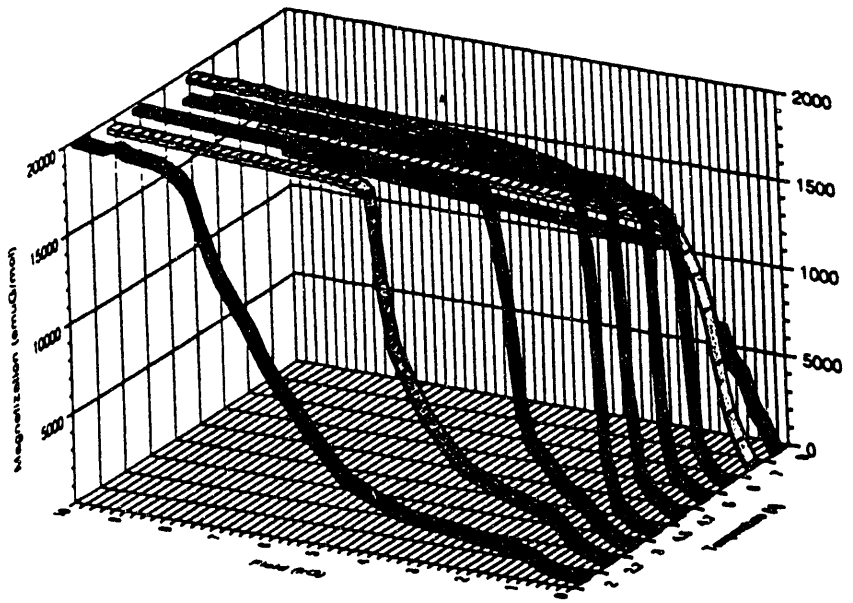

Figure 12 (B). $M_1(H)$ for zero field cooled samples at different T.

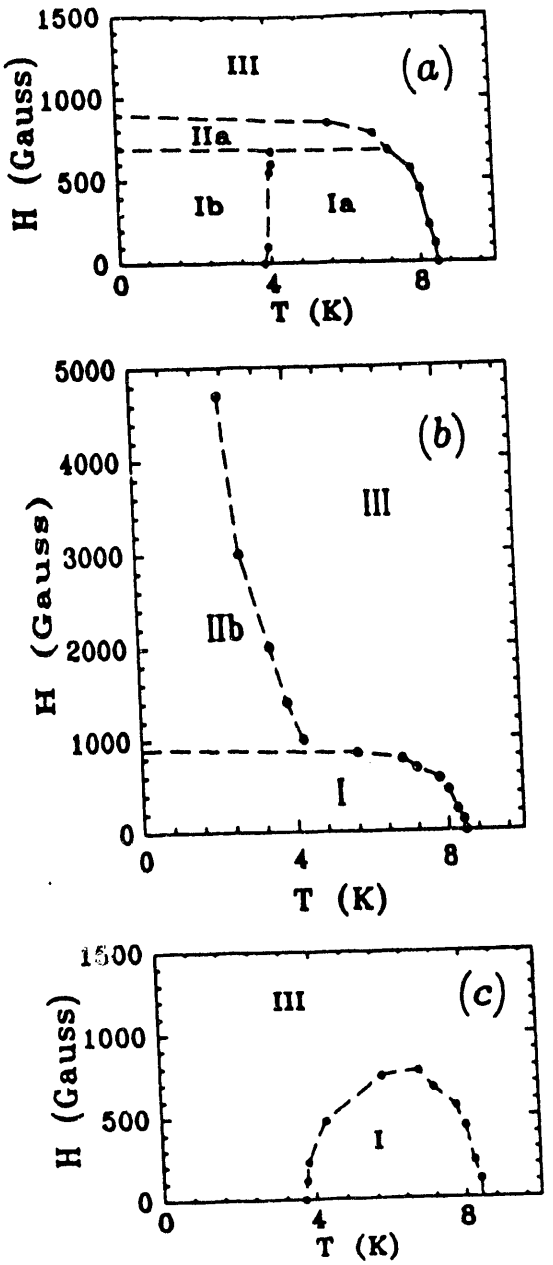

Figure 12 (C). Phase diagrams of [$MnCp^*_2$][DDQ]. (a) Equilibrium phase diagram obtained from (A) I-AFM, IIa - Mixed phase, III-FM phase; (b) Non-equilibrium phase diagram obtained from M vs H (increasing H) at different temperatures, Figures (A) and (B). I-AFM phase, IIb - Field induced intermediate phase, III - Field induced FM phase; (c) Non-equilibrium phase diagram obtained from M vs T (increasing T) at different resident field (field reduced from FM phase), I-AFM phase, III-Field induced FM phase.

iii. Models of magnetic exchange and magnetic phenomena

- *Preliminary model for magnetism in $V(TCNE)_x{\cdot}y(CH_2Cl_2)$.* From infrared and elemental analyses we formulate this material as $V^{II}((TCNE)_2 1/2(CH_2Cl_2)$ with S = 3/2 V^{II}, and S = 1/2 $[TCNE]^{\cdot-}$ ligands. Antiferromagnetic coupling between the two [TCNE] S = 1/2 spins and the vanadium S = 3/2 (net ferrimagnetic behavior) results in a predicted saturation moment of 5.6×10^3 emuG/mol in agreement with the measured value of 6.0×10^3 emuG/mol observed at 2K for an applied magnetic field of 19.5 kG.
- *Decrease of ferromagnetic T_C with increasing spin defect concentration.* The rate of decrease of T_c with concentration of spinless sites in a chain was determined to be of the order of the exchange spatial anisotropy (*i.e.*, $J_{interchain}/J_{intrachain}$) of the parent system in accordance with long standing theoretical predictions [12]. These results demonstrate that the preparation of high spin oligomers is insufficient to create 3-D magnetic solids, because high spin oligomers can be mapped onto a model of infinite chains with spinless defects. Hence these studies demonstrate that one needs to have very long chains of magnetic molecules if one is dealing with highly anisotropic exchange interactions.
- *A 3-D mean field model for T_C of a two-site system was developed.* This mean field model is used to correctly predict the increase in T_c in replacing $[FeCp^*_2]^{+\cdot}$(S = 1/2) with $[MnCp^*_2]^{+:}$ (S = 1) in an isomorphous structure. The predicted increase of T_c of 86% was subsequently verified by experiment (83% increase of T_c) (with D. Dixon and A. Suna, Du Pont).
- *A Monte Carlo model was developed to account for complex metamagnetic behavior of $[MnCp^*_2]^{+:}[DDQ]^{\cdot-}$.* Results supported a crossover from isolated to cooperative spin flipping below 4K.

END

DATE
FILMED
3/31/93